Exhibit A

Immunity, Vol. 17, 693–702, December, 2002, Copyright ©2002 by Cell Press

Real-Time Visualization of *Mycobacterium*-Macrophage Interactions Leading to Initiation of Granuloma Formation in Zebrafish Embryos

J. Muse Davis,[1] Hilary Clay,[3]
Jessica L. Lewis,[3] Nafisa Ghori,[4]
Philippe Herbomel,[5,6] and Lalita Ramakrishnan[1,2,6]
[1]Department of Microbiology
[2]Department of Medicine
[3]Molecular and Cellular Biology Graduate Program
University of Washington School of Medicine
Seattle, Washington 98195
[4]Electron Microscopy Center
Stanford University School of Medicine
Stanford, California 94305
[5]Unité Macrophages et Développement de l'Immunité
Institut Pasteur
75015 Paris
France

Summary

Infection of vertebrate hosts with pathogenic Mycobacteria, the agents of tuberculosis, produces granulomas, highly organized structures containing differentiated macrophages and lymphocytes, that sequester the pathogen. Adult zebrafish are naturally susceptible to tuberculosis caused by *Mycobacterium marinum*. Here, we exploit the optical transparency of zebrafish embryos to image the events of *M. marinum* infection in vivo. Despite the fact that the embryos do not yet have lymphocytes, infection leads to the formation of macrophage aggregates with pathological hallmarks of granulomas and activation of previously identified granuloma-specific *Mycobacterium* genes. Thus, *Mycobacterium*-macrophage interactions can initiate granuloma formation solely in the context of innate immunity. Strikingly, infection can redirect normal embryonic macrophage migration, even recruiting macrophages seemingly committed to their developmentally dictated tissue sites.

Introduction

Infection with pathogenic Mycobacteria results in a hallmark host response, specifically the formation of granulomas, highly organized structures characterized by the presence of differentiated macrophages that contain but fail to eradicate the pathogen (Dannenberg, 1993; Flynn and Chan, 2001). Even early after infection, tuberculous granulomas are complex, consisting of highly differentiated, tightly interdigitated macrophages referred to as epithelioid cells, as well as T lymphocytes and other immune cells (Dannenberg, 1993; Flynn and Chan, 2001; Roach et al., 1999). For instance, in a mouse model of *M. bovis* BCG infection, aggregates of eight to ten macrophages, first detected at 2 weeks postinfection, already contained CD4+ T lymphocytes (Roach et al., 1999). Therefore, it has been difficult to dissect the roles of individual host factors and cells that mediate granuloma formation and their influence on infection outcomes (Flynn and Chan, 2001).

M. marinum, a close genomic relative of *Mycobacterium tuberculosis*, the agent of human tuberculosis (Tonjum et al., 1998) (http://www.sanger.ac.uk/Projects/M_marinum), causes tuberculosis in ectotherms (Clark and Shepard, 1963) and superficial granulomatous infection in humans (Travis et al., 1985). *M. marinum*, like other pathogenic Mycobacteria, produces chronic infection of macrophages resulting in tuberculous granulomas, making it a useful model to study fundamental mechanisms of *Mycobacterium* pathogenesis (Barker et al., 1997; Bouley et al., 2001; Chan et al., 2002; Ramakrishnan et al., 1997; Talaat et al., 1998).

Our understanding of the mechanism and role of granuloma formation during tuberculous infection would benefit from an experimental model in which the sequence of early pathogen-macrophage interactions resulting in granulomas can be delineated. The zebrafish is a genetically tractable vertebrate (Golling et al., 2002; Haffter et al., 1996; Nasevicius and Ekker, 2000; Patton and Zon, 2001; Wienholds et al., 2002) and a choice model organism for the study of vertebrate development and disease (Dooley and Zon, 2000; Fishman, 2001). The imminent completion of its genome sequence (http://www.ensembl.org/Danio_rerio/) adds to its attractiveness as a model host. Close homologs of several key human and mouse immune molecules such as immunoglobulin light chains, β2-microglobulin, T cell antigen receptors, Rag 1 and 2, MHC Class I and II, and complement factors have already been identified (Haire et al., 2000; Ono et al., 1993, 1992; Seeger et al., 1996; Takeuchi et al., 1995; Willett et al., 1997). Therefore we sought to determine if zebrafish, a natural host for *M. marinum*, could be used to dissect early host responses to tuberculosis.

While the adult zebrafish is known to be susceptible to *M. marinum* (Westerfield, 2000), it is the embryo and early swimming larvae that are optically transparent (Kimmel et al., 1995), potentially allowing close monitoring of host-pathogen interactions in vivo. (Henceforth, we will refer to both embryos and early swimming larvae as embryos.) Furthermore, the embryo is more susceptible than the adult to genetic manipulations: specific genes can be functionally inactivated in the embryo using antisense oligonucleotide technology (Nasevicius and Ekker, 2000). Broad-based genetic screens are also more feasible in embryos (Golling et al., 2002; Haffter et al., 1996; Wienholds et al., 2002).

For these reasons, we wished to determine if the embryos, like adult zebrafish, were also susceptible to *M. marinum* infection. This seemed likely in light of our previous discovery that zebrafish embryos, like other vertebrate embryos, have early macrophages that differentiate in the yolk sac before other leukocytes arise (Herbomel et al., 1999) (Figure 1A). These early macrophages migrate rapidly into the mesenchyme and developing organs and vasculature (Herbomel et al., 1999, 2001), thus providing a potential niche for macrophage

[6]Correspondence: lalitar@u.washington.edu (L.R.), herbomel@pasteur.fr (P.H.)

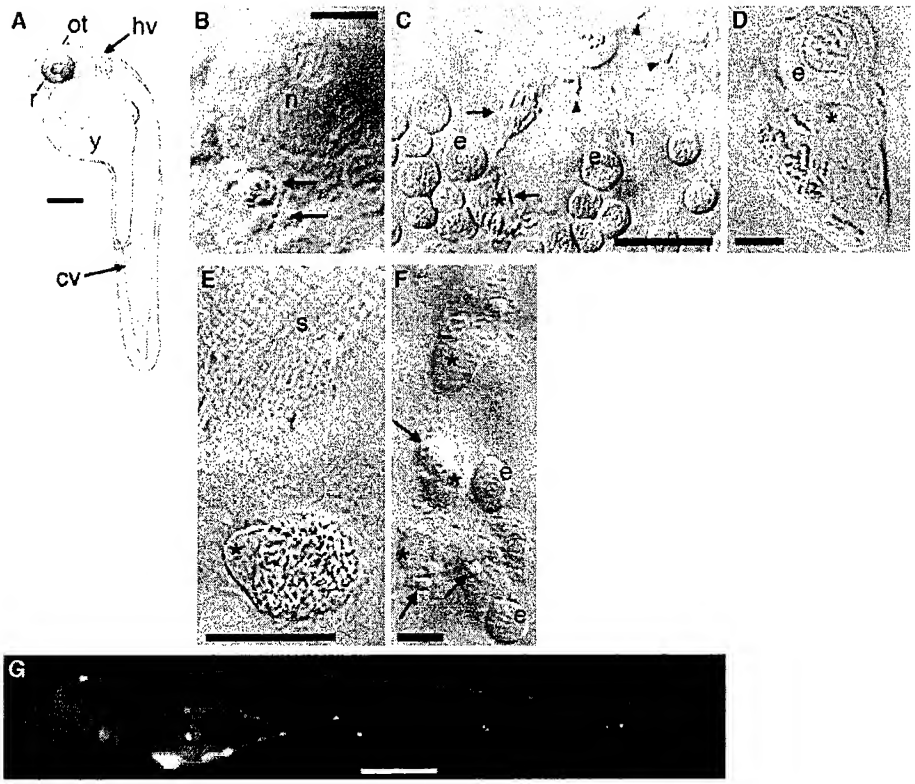

Figure 1. *M. marinum* and *S. arizonae* Infection of Zebrafish Embryos

(A) Landmarks in the zebrafish embryo at 32 hr pf (Kimmel et al., 1995). Red arrows show the path of blood flowing over the yolk (y). Arrows show the two injection sites used in this study: caudal vein (cv) and hindbrain ventricle (hv); r, retina, ot, optic tectum. Bar, 200 μm.

(B) Overlay of fluorescence and DIC images of 5 day pf embryo infected by coincubation with fluorescent *M. marinum* showing two macrophages (arrows) containing fluorescent bacteria, in the epidermis close to a neuromast (n). Bar, 25 μm.

(C) DIC image of an embryo injected intravenously at 32 hr pf with *M. marinum*, showing the yolk sac circulation valley, taken 1 hr pi. Two macrophages (arrows) have phagocytosed several bacteria; free bacteria (arrowheads) are still visible in the blood. Asterisks indicate nuclei of macrophages. e, erythroblast. Bar, 25 μm.

(D) Higher magnification DIC image of the yolk sac circulation valley of an embryo from (C) showing an infected macrophage in close contact with an erythroblast (e). Asterisk, macrophage nucleus. Bar, 5 μm.

(E) DIC images of an embryo injected intravenously at 32 hr pf with *M. marinum*, taken 6 days pi showing an infected macrophage in trunk epidermis just superficial to striated muscle (s). Asterisk, macrophage nucleus. Bar, 25 μm.

(F) DIC image of yolk sac circulation valley, 4 hr after injection of *S. arizonae* at 32 hr pf showing four infected macrophages. White arrow points to a spacious phagosome containing four motile bacteria (motility was determined by video microscopy), which are only partially visible at this focal plane. Black arrows mark localized protuberances. Asterisks mark macrophage nuclei; e, erythroblasts. Bar, 10 μm.

(G) Fluorescence image of a whole embryo 120 hr after injection of nine fluorescent *M. marinum* at 32 hr pf. Fluorescence in head, yolk region, and tail indicates disseminated infection. Bar, 400 μm.

pathogens such as *Mycobacterium*. Zebrafish embryonic macrophages can quickly eradicate a massive inoculum of nonpathogenic bacteria (Herbomel et al., 1999), demonstrating their competence in combating infections.

In this study, we demonstrate that *M. marinum* causes a systemic infection in zebrafish embryos with key characteristics of adult Mycobacterioses, namely the aggregation of macrophages into granuloma-like structures and the activation of *M. marinum* granuloma-specific genes. In addition, we show that infection impacts normal macrophage migration and differentiation during embryonic development.

Results

Infection of Embryonic Macrophages with *M. marinum*

We first infected zebrafish embryos by incubating them at 5 hr postfertilization (pf) with *M. marinum* rendered fluorescent by expression of various *M. marinum* promoters fused to the Green Fluorescent Protein gene (*gfp*) (Chan et al., 2002). Infected macrophages were observed in the embryo by 5 days pf (Figure 1B). To analyze the early events of infection by fluorescence and Differential Interference Contrast (DIC) video microscopy, we injected *M. marinum msp*12::*gfp*, a consti-

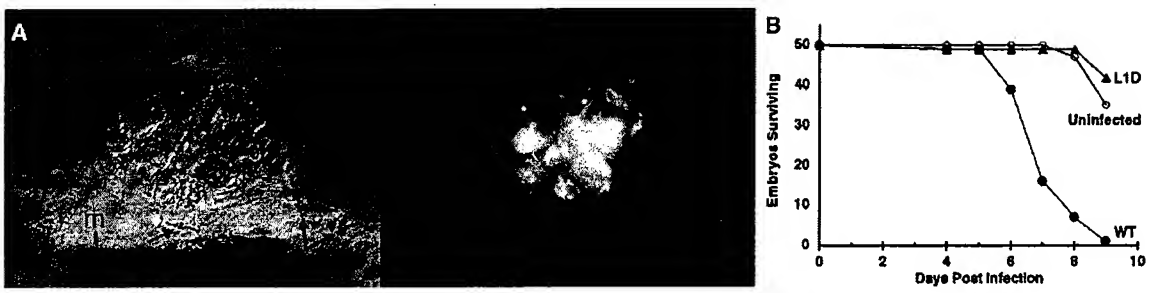

Figure 2. Aggregate Formation in and Survival of *M. marinum*-Infected Embryos

(A) DIC (left) and corresponding fluorescence image (right). 4 days pi, tight macrophage aggregate in tail (ventral up position), between caudal vein and epidermis; asterisk marks an infected macrophage at the periphery of an aggregate; arrows indicate bacteria in two other macrophages nearby. m, melanocyte, s, striated muscle. Bar, 25 μm.

(B) Survival curve for embryos intravenously infected with 619 ± 61 wild-type (WT) or 674 ± 86 L1D strains of *M. marinum*.

tutively fluorescent strain, into the caudal vein at 32 hr pf (Figure 1A) (Chan et al., 2002; Westerfield, 2000). Phagocytosis by blood macrophages occurred immediately postinjection (pi) (Figures 1C and 1D).

Individual infected macrophages, often motile, were detected in diverse tissues by 1 day pi, indicating their extravasation from the blood (Figure 1E; also see Supplemental Movie S1 at http://www.immunity.com/cgi/content/full/17/6/693/DC1). Early events captured by video microscopy included instances of bacterial transfer between two macrophages through membrane tethers, and an uninfected tissue macrophage phagocytosing a dead (nonmotile) infected macrophage, processes that may constitute new mechanisms of bacterial dissemination during early infection (see Supplemental Movies S2 and S3 at http://www.immunity.com/cgi/content/full/17/6/693/DC1). Consistent with our observations of bacterial dissemination by macrophages, intravenous injection of as few as nine bacteria established systemic infection (Figure 1G). Interestingly, other cell types did not appear to phagocytose *M. marinum*.

Formation of Granuloma-like Aggregates Soon after *M. marinum* Infection

At 3 days pi, the infected macrophages that had extravasated into the tissues began to form tight aggregates (Figures 2A, 4E, and 6A). Video microscopy revealed the dynamic nature of these aggregates: we observed continuous squeezing movements of the tightly apposed membranes of aggregated cells as well as individual cells migrating into the aggregates (see Supplemental Movie S4 at http://www.immunity.com/cgi/content/full/17/6/693/DC1).

Transmission electron microscopy confirmed that the aggregates consist of a homogeneous cell type. The aggregated cells had large euchromatic nuclei characteristic of activated macrophages (Adams, 1976; Bouley et al., 2001). They also had either tightly apposed cell membranes (Figure 3A) or indistinct cell boundaries (Figure 3B), features seen, respectively, in epithelioid cells and multinucleated giant cells in established granulomas (Adams, 1976). Both infected and uninfected cells were found, as they are in established tuberculous granulomas (Figures 3A and 3B) (Bouley et al., 2001; Dannenberg, 1993). As in adult tuberculous granulomas (Bouley et al., 2001; Dannenberg, 1993; Talaat et al., 1998), bacteria were intracellular (Figure 3A), sequestered tightly by cellular aggregates (Figure 3B), or extracellular, in large necrotic foci (Figure 3C). Different infected foci contained vastly different numbers of bacteria (compare [B] and [C] in Figure 3), suggesting differences in local outcomes to infection.

To validate further this infection model, we compared the fate of live and heat-killed wild-type bacteria as well as an attenuated mutant bacterial strain in the embryos. Embryos injected with >500 *M. marinum* died between 6–9 days postinfection (Figure 2B), whereas most injected with <20 bacteria had a lower level of infection and survived during the 9 day monitoring period (data not shown). Comparable numbers of heat-killed bacteria were readily phagocytosed by the macrophages but were degraded within 2 days pi. We also infected embryos with the *M. marinum* L1D mutant strain that is attenuated in granulomatous infection of adult frogs (Ramakrishnan et al., 2000). Infection of adult animals with this strain results in a reduced bacterial burden and fewer granulomas that are often composed of loose macrophage aggregates (Bouley et al., 2001; Ramakrishnan et al., 2000). The L1D strain was also found to be attenuated during zebrafish embryonic infection: it failed to kill the embryos even at high inocula (Figure 2B), and there was a corresponding reduction in bacterial load and very few infectious foci as compared to wild-type infection (data not shown).

Salmonella arizonae Infection Produces a Distinct Phenotype in Zebrafish Embryos

To determine if the observed interactions of zebrafish embryonic macrophages with *M. marinum* were pathogen specific, we examined the course of infection with *Salmonella arizonae*, another facultative intracellular pathogen of ectotherms (Bartlett et al., 1977). The infected macrophages had a distinct phenotype of localized protuberances and motile bacteria within spacious phagosomes (Figure 1F), similar to that seen in adult-derived cultured macrophages infected with *Salmonella* (Alpuche-Aranda et al., 1994). Furthermore, video microscopy revealed that infected cells in the embryos

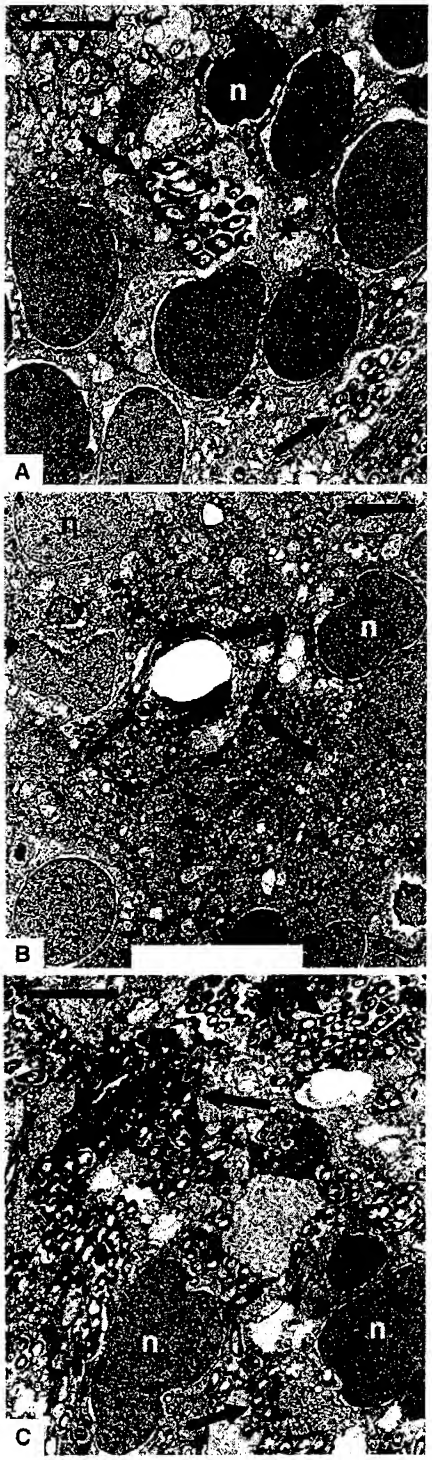

Figure 3. Transmission Electron Micrographs of *M. marinum*-Induced Aggregates

(A) Cellular aggregate with intracellular bacteria probably within the cell whose nucleus is marked (n). Asterisks denote tight intercellular membranes.

(B) Multiple host cell nuclei with no discernible cell membranes surround a few bacteria within an apparent wall or membrane (arrow). Tear (white oval) in region of bacteria is an artifact (Bouley et al., 2001).

(C) Many bacteria in an area of acellular necrotic debris with two host cell nuclei at bottom. Bars, 3 μm. n, cell nuclei; arrows indicate bacteria.

were often found to lyse within an hour of infection (data not shown). This early lysis of infected cells has been observed during *Salmonella* infection of cultured macrophages (Brennan and Cookson, 2000; Monack et al., 2001). In contrast to *M. marinum* infection, injection of 5–20 *S. arizonae* was lethal within 48 hr. These data confirm that the embryos, like adult animals, react to different intracellular pathogens in distinct ways.

Induction of *M. marinum* Granuloma-Activated Genes in Aggregates

We previously identified *M. marinum* genes that are activated only when the bacteria reside in adult frog granulomas by screening a library of *M. marinum* promoter fusions to *gfp* (Chan et al., 2002; Ramakrishnan et al., 2000). A few of these genes, referred to as macrophage-activated genes (*mag*s), are also activated upon infection of individual cultured macrophages. However, most of them, termed granuloma-activated genes (*gag*s), are activated only in granulomas and not in cultured macrophages or other in vitro conditions predicted to mimic aspects of the granuloma environment (Chan et al., 2002). These results suggest an orchestrated sequence of host-induced *M. marinum* gene activation with some genes activated upon phagocytosis and others requiring complex cues from the granuloma environment.

To determine whether the microenvironment of the *M. marinum*-induced aggregates in zebrafish embryos has the properties of adult granulomas, we monitored the expression of *mag*s and *gag*s during infection. All four *M. marinum mag*s tested were activated soon after phagocytosis by individual macrophages (Figures 4A–4C and 5). In contrast, the three *gag*s tested were activated only upon aggregation of infected macrophages (Figures 4D and 4E). It was possible that the fluorescence seen in the aggregates was only an artifact of many dimly fluorescent bacteria (whose *gag* fusions were not activated) clustered together appearing to be highly fluorescent. To exclude this possibility, the fluorescence of individual bacteria that had been in the embryonic aggregates (see Experimental Procedures for details of their isolation from the aggregates) was compared to the fluorescence of individual bacteria grown in liquid medium or in cultured macrophages (Figure 5). Specific activation of the *M. marinum gag*s in the context of embryonic macrophage aggregates was confirmed. The quantification of fluorescence values of the *M. marinum mag* and *gag* fusions under the three different conditions is presented in Supplemental Table S1 (http://www.immunity.com/cgi/content/full/17/6/693/DC1).

In summary, these results show that the macrophage aggregates in the embryo resemble adult granulomas not only in their histological features but also in their ability to activate *gag*s. Furthermore, we have been able to refine our analysis of the *mag*s and *gag*s in the zebra-

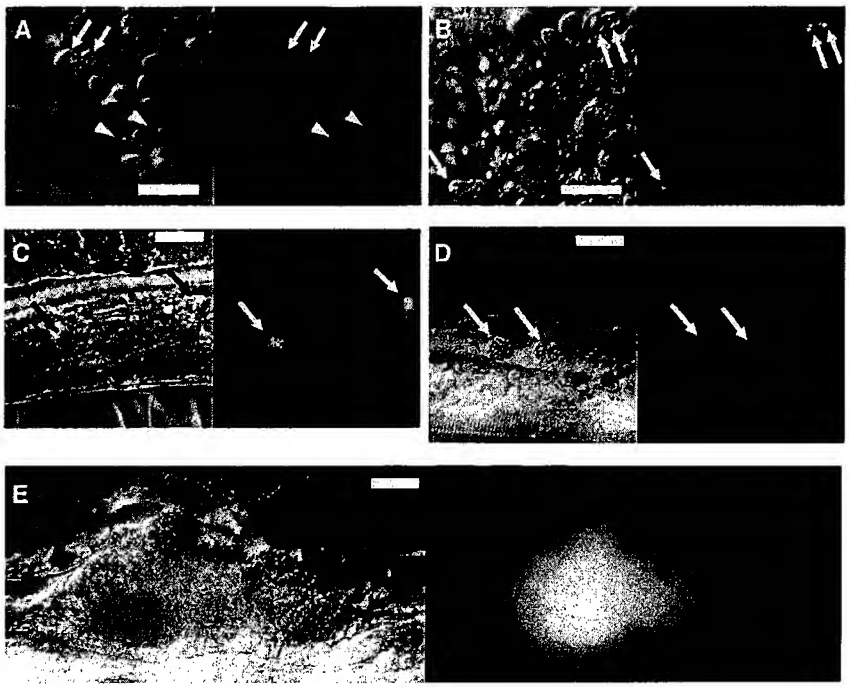

Figure 4. Expression of *M. marinum mag*s and *gag*s in Embryos

DIC and corresponding fluorescence images. (A–B) *M. marinum mag* 85::*gfp*. (A) Yolk sac, 30 min pi. Faintly fluorescent bacteria within macrophages (arrows) and nonfluorescent extracellular bacteria (arrowheads). (B) Yolk sac of the same embryo 2 hr pi. All bacteria (arrows) are in macrophages and highly fluorescent.

(C) *M. marinum mag* 25::*gfp* 2 hr pi. Individual infected macrophages in the tail are highly fluorescent (arrows).

(D and E) *M. marinum gag*7::*gfp* 5 days pi showing nonfluorescent individual macrophages (D, arrows) and a brightly fluorescent macrophage aggregate nearby (E). Bars, 25 μm.

fish embryo. *mag* 25, whose *M. tuberculosis* homolog (*whiB*3) is a virulence determinant (Steyn et al., 2002), straddles the *mag* and *gag* categories in adult infection, being slightly activated in cultured macrophages and much more highly activated in adult granulomas (Chan et al., 2002). While the activation of *mag* 25 remained at a low level in activated cultured macrophages (by addition of interferon-γ and T cell supernatants derived from tuberculous infection) (Chan et al., 2002), it was strongly activated in zebrafish embryos soon after infection of individual macrophages (Figures 4C and 5). This result reveals that the macrophage intracellular microenvironments that exist in vivo represent a wide spectrum, much more complex than can be elicited in vitro.

Recruitment of Macrophages to Sites of Infection by an M-CSF-R-Independent Pathway

In our infections, zebrafish embryonic macrophages migrate toward *M. marinum* and participate in granuloma formation at a developmental stage when they are

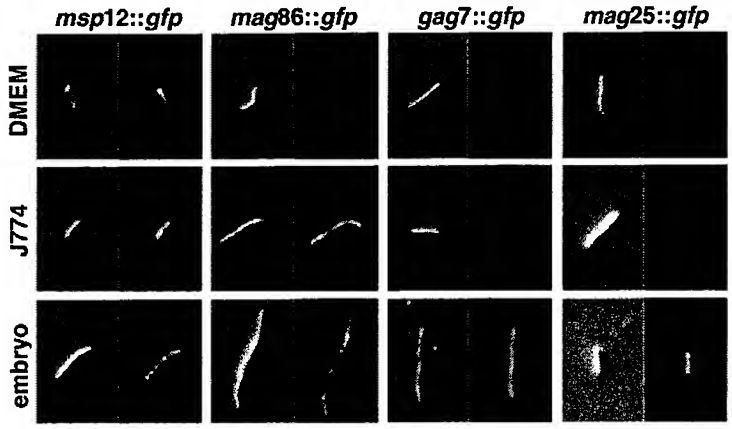

Figure 5. Fluorescence of Individual Bacteria from DMEM Medium, J774 Macrophages, and Embryo Granulomas

For each column, the left panel is the DIC image and the right panel is the fluorescence image. Note that *msp* 12::*gfp*, a constitutive promoter, is expressed at the same level in all three conditions, *mag* 86::*gfp* is activated in both J774 cells and in the embryo, and *gag*7::*gfp* is activated only in the aggregates of the infected embryo. *mag* 25::*gfp* is slightly activated in J774 cells and more activated in the embryo.

Figure 6. *M. marinum* Infection of *panther* Embryos

(A) Aggregate resulting from *M. marinum gag7::gfp* infection protruding from body wall (b). Left panel, DIC; right panel, corresponding fluorescence. m, melanocyte.

(B) DIC and fluorescence overlay image of hindbrain ventricle (lateral view, anterior to the left) of a *panther* embryo injected with ~20 bacteria at 32 hr pf and viewed 1 hr pi showing infected macrophages adherent to the dorsal wall (roof) of the ventricle (arrows) and free bacteria (arrowheads). Bar, 50 μm.

normally targeted to specific embryonic tissues by a Macrophage Colony Stimulating Factor Receptor (M-CSF-R)-dependent pathway (Herbomel et al., 2001). *M. marinum*-induced macrophage recruitment was underscored by the finding that injection of 20–100 bacteria into the embryos' hindbrain ventricle (Figure 1A) at 32 hr pf resulted in rapid arrival of macrophages from distant sites in the body (data not shown). Given the capacity of embryonic macrophages to migrate in response to both developmental cues and the presence of bacteria, we investigated the pathway of *M. marinum*-induced macrophage migration and the potential interference of infection with development.

We first employed zebrafish *panther* embryos, which lack a functional M-CSF-R (Parichy et al., 2000), to determine if macrophage migration in response to *M. marinum*, like their developmental migration, is mediated by an M-CSF-R-dependent pathway. Early macrophages in *panther* embryos appear to differentiate normally in the yolk sac but exhibit delayed colonization of the head (Herbomel et al., 2001). We found that *panther* embryos injected intravenously with *M. marinum* exhibited granuloma formation and *gag* activation similar to wild-type embryos (Figure 6A). To evaluate more stringently the migratory capacity of *panther* macrophages in response to *M. marinum*, we injected ~20 bacteria into the hindbrain ventricle (Figure 1A) at 32 hr pf, when macrophages are absent from the entire head of these mutant embryos (Herbomel et al., 2001). Yet, in *panther* embryos, as in wild-type, macrophages were recruited to the infected ventricle within 1 hr pi (Figure 6B). Thus, *M. marinum* recruits macrophages by a pathway(s) distinct from that involved in macrophage colonization of the head during development.

M. marinum Infection Redirects the Developmental Program of Embryonic Macrophage Migration

M-CSF-R-dependent developmental migration of macrophages is highlighted by their heavy colonization of the midbrain optic tectum between 60–84 hr pf (Herbomel et al., 2001). After entering the brain, these macrophages undergo a distinct phenotypic transformation into early microglial cells that express high levels of Apolipoprotein E, a neurotrophic lipid carrier. These differentiated macrophages/early microglia phagocytose the numerous apoptotic bodies that appear in the brain at this stage (Herbomel et al., 2001). Therefore, we next asked if blood infection with *M. marinum* would prevent macrophage colonization of the tectum and the subsequent phagocytosis of apoptotic bodies. Injection of bacteria into the caudal vein of embryos at 32 hr pf led to a dramatic reduction of early microglial cells (data not shown) and a correlative accumulation of apoptotic bodies in the tectum at 72–120 hr pf, proportional to the level of infection (Figures 7A and 7B). Finally, we asked if blood infection with *M. marinum* would cause the tectum macrophages that had already differentiated into microglial cells to leave the brain to join sites of infection. We injected ~500 bacteria into the caudal vein of 72 hr pf embryos. At 144 hr pf, when infection had progressed to involve many blood and mesenchymal macrophages (Figure 7E), there was a striking decrease in microglial cell numbers in the tectum (36 ± 2 for uninfected versus 9 ± 3 for infected, $p < 0.001$, see Experimental Procedures for details). This finding, coupled with our failure to visualize dead cells in the area, suggests these microglial cells had left the brain to join infection foci in the tissues (Figures 7C and 7D). This reverse trafficking of microglial cells in response to infection occurred despite their phenotypic transformation in the brain. Therefore, even seemingly committed brain macrophages/microglia return to their primitive roots upon challenge with infection.

Discussion

Here, we have demonstrated the feasibility and validity of the zebrafish embryo model for understanding early host responses to tuberculous infection. *M. marinum* elicits specific host responses in the embryos, which mimic those of adult animals (Bouley et al., 2001; Ramakrishnan et al., 1997; Talaat et al., 1998). Infection results in the formation of tight macrophage aggregates with distinctive features of mature adult granulomas in that the participating macrophages have differentiated into epithelioid and multinucleated cells (Adams, 1976; Bouley et al., 2001; Dannenberg, 1993). The *M. marinum* L1D strain, attenuated in adult granulomatous infection (Bouley et al., 2001; Ramakrishnan et al., 2000), is also attenuated during embryonic infection, further validating this system.

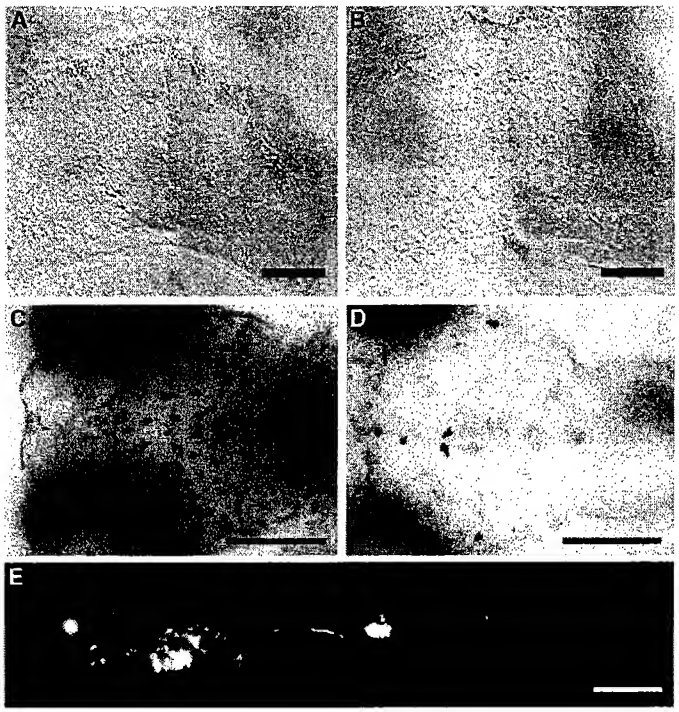

Figure 7. Interference of *M. marinum* Infection with Macrophage Developmental Migration

(A–D) DIC images. (E) fluorescence image.

(A and B) Midbrain optic tectum of 72 hr pf embryos after intravenous injection of *M. marinum msp* 12::*gfp* at 32 hr pf. Dorsal view, anterior up. (A) Lightly infected embryo, with few apoptotic bodies visible. (B) Heavily infected embryo, with accumulated apoptotic bodies. Bars, 50 μm.

(C and D) Neutral red staining of macrophages in 144 hr pf embryos after injection of bacteria at 72 hr pf. Dorsal view, anterior to left. Bars, 200 μm. (C) Optic tectum of uninfected embryo. (D) Optic tectum of infected embryo whose level of overall infection is shown in (E). Bar in (E), 400 μm.

The zebrafish embryo has provided a unique system to visualize the nuances of host-*Mycobacterium* interactions and monitor the progression of the pathological consequences of infection in a live organism. Our study reveals two new mechanisms of bacterial dissemination mediated by macrophages: direct transfer between macrophages via intercellular tethers, and re-phagocytosis of bacteria associated with dead macrophages in tissues. We have made direct observations of the dynamic nature of even tightly knit granuloma-like aggregates, as well as uninfected macrophages recruited from afar into the granuloma.

Perhaps most striking of all is our finding that some *M. marinum* genes activated specifically in adult granulomas (Chan et al., 2002; Ramakrishnan et al., 2000) are also activated specifically upon formation of the embryonic macrophage aggregates. This last result confirms that the complex environmental cues inducing bacterial gene expression in adult granulomas are also present in the embryonic aggregates. It also reveals the difference in the intracellular environment between single infected macrophages and aggregated ones. The aggregated macrophages clearly must have undergone changes in their microenvironment, perhaps as a result of cell-cell signaling, that trigger activation of the *M. marinum gag*s. Future use of this model will help to clarify the origin of these changes and will determine if other *M. marinum gags* require further maturation of these aggregates for their activation.

Our discovery of *M. marinum*-induced granuloma-like aggregates in zebrafish embryos has important implications for the study of host factors required at various stages of granuloma formation and maturation. While the pathological definition and staging of granulomas is based on the formation of macrophage aggregates and their specialized differentiation (Adams, 1976), tuberculosis researchers consider granulomas to be structures that also include other cells such as lymphocytes and dendritic cells (Dannenberg, 1993; Flynn and Chan, 2001). Previous studies using adult mammalian hosts have implicated components of adaptive immunity, principally T lymphocytes, in the recruitment and activation of macrophages to form *Mycobacterium* granulomas and contain infection (Dannenberg, 1993; Flynn and Chan, 2001; Kaufmann and Ladel, 1994; North and Izzo, 1993). However, studies on *M. tuberculosis* infection of either gene-disrupted or antibody-depleted mice suggest that the early aggregation of macrophages is promoted by tumor necrosis factor α (TNF-α), a cytokine made principally by macrophages. In contrast, in the absence of interferon-γ, a cytokine made principally by T lymphocytes, mice do initiate macrophage aggregations, but these structures rapidly become necrotic and devoid of mononuclear cells (Bean et al., 1999; Cooper et al., 1993; Flynn and Chan, 2001; Flynn et al., 1993, 1995). The exact contribution of the various immune components to the formation of granulomas and their ability to control bacterial growth remains enigmatic.

While the zebrafish has a complex innate and adaptive immune system akin to that of mammals (Trede et al., 2001), its embryos and early swimming larvae lack elements of adaptive immunity. Lymphoblasts first colonize the thymus at 65 hr pf, and T lymphocytes are not yet circulating at 4 days pf (Trede et al., 2001; Willett et al., 1999). By this time, granuloma-like aggregates have already formed in the infected embryos. Therefore, our results suggest that the pathognomonic adult response to *M. marinum*—the formation of tight aggregates of

highly differentiated macrophages (epithelioid cells) and multinucleated cells surrounding bacteria—is shaped without the involvement of adaptive immunity. Furthermore, *M. marinum* infection was found to produce identical macrophage aggregates with *gag* activation in zebrafish mutant embryos that have thymic hypoplasia resulting in a complete absence of T lymphocytes, but normal myeloid and erythroid lineages (J.M.D., N. Trede, L. Zon, and L.R., unpublished data). This finding further supports the idea that initiation of granuloma-like aggregates and differentiation of macrophages into epithelioid cells is independent of T lymphocytes. It is possible that the components of innate immunity, such as the infected macrophages themselves, NK cells, or dendritic cells, are mediating the production of interferon-γ (Fenton et al., 1997; Flynn and Chan, 2001; Wang et al., 1999). Future experiments with this model will probe the role of interferon-γ and TNF-α during embryonic infection and determine the timing of NK and dendritic cell differentiation.

While it appears that pathological structures resembling adult granulomas are formed rapidly following *M. marinum* infection of embryos, the question remains as to how potent the microbicidal capacity of these aggregates is in the absence of an adaptive immune response. Our electron micrographs show variability in bacterial numbers in different infected regions (Figure 3). Some areas appear to have an effective local host response consisting of many host cells and very few bacteria (Figures 3A and 3B), much like chronic granulomas in *M. marinum*-infected adult frogs (Bouley et al., 2001; Ramakrishnan et al., 1997). Others have a more necrotic appearance with numerous bacilli, more like adult granulomas from an immunodeficient host (Cooper et al., 1993; Flynn et al., 1993, 1995; Ramakrishnan et al., 1997). Furthermore, sequential monitoring of infected embryos has revealed different local outcomes to infection within the same embryo, with some aggregates enlarging while others in the same embryo are shrinking, with concomitant loss of viability of the bacteria within them (O. Humbert, J.M.D., and L.R., unpublished data). This result would suggest differences in the local host responses of the embryo and that the host responses mounted in the absence of the adaptive immune response are capable of at least some microbicidal activity. There is evidence for the role of innate immune mechanisms in clearing Mycobacteria in both animal and human studies (van Crevel et al., 2002).

Undoubtedly, intervention by the adaptive immune system modulates the process further, potentially accounting for the more uniformly paucibacillary infections seen in immunocompetent adult hosts (Bouley et al., 2001; Dannenberg, 1993; Ramakrishnan et al., 1997; Talaat et al., 1998), in contrast to the multibacillary nature of many of the embryonic aggregates. We are now able to raise some infected embryos into adult fish (D. Beery and L.R., unpublished data), allowing the study of the impact of the adaptive immune response, particularly T lymphocyte development, on the infection phenotype.

Another important finding of this study is that recruitment of macrophages by *M. marinum* is mediated by a pathway independent of M-CSF-R, a receptor normally involved in their developmental migration during this stage (Herbomel et al., 2001). It is possible that the zebrafish has multiple paralogous M-CSF-R genes, providing functional redundancy in signals mediating macrophage recruitment to sites of infection. Even if that proves to be the case, our results with the *panther* mutant, where developmental macrophage migration is affected while migration in response to bacteria is not, suggest that distinct pathways of macrophage migration are operant at this stage. M-CSF is a known chemoattractant of macrophages (Webb et al., 1996), and has been found to impact the ultimate outcome of tuberculosis in an adult mouse model of infection (Teitelbaum et al., 1999). Coupled with that study, our results would suggest that M-CSF may mediate subsequent signaling events during infection rather than the initial ones recruiting macrophages to the site of infection and causing their aggregation into granulomas.

Strikingly, infection redirects normal migration and differentiation of embryonic macrophages. The finding that cues from an infection can override normal developmental cues has implications for human fetal developmental abnormalities associated with intrauterine infections by intracellular pathogens such as *Toxoplasma gondii* (Remington et al., 1994).

Studies using genetically tractable invertebrates such as *Drosophila* and *C. elegans* have been used to elucidate mechanisms of host-pathogen interactions resulting in disease (Michel et al., 2001; Ramet et al., 2002; Tan and Ausubel, 2000). Their use has yielded important insights into the mechanisms by which the innate immune system recognizes pathogens (Kim et al., 2002; Michel et al., 2001; Ramet et al., 2002). In this work, we have used zebrafish embryos to demonstrate that innate immunity is sufficient to initiate granuloma formation in response to pathogenic Mycobacteria. Not only does the zebrafish allow the study of infectious processes by real-time visualization, but the presence of both innate and adaptive immune systems in this genetically tractable vertebrate will allow dissection of how the two arms of the immune system interface with each other to combat infection.

Experimental Procedures

Bacterial Cultures and Maintenance and Infection of Embryos

Zebrafish embryos were kept in embryo medium for 12 hr pf and then moved to 0.003% Phenyl-Thiourea in embryo medium to prevent melanization (Westerfield, 2000). For infection by coincubation, nondechorionated, 4 hr pf embryos were incubated for 4 days at 28°C in 10 ml of embryo medium containing ~10^7 *M. marinum*. At this temperature, the embryos hatch at 50–55 hr pf, at which point it is likely that they become accessible to the bacteria. Injections of embryos were performed as described (Westerfield, 2000). Logarithmic phase *M. marinum* cultures bearing various fluorescent reporter constructs grown in liquid medium (Chan et al., 2002), and stationary phase *S. arizonae* liquid cultures, were resuspended in embryo medium containing 1% phenol red to aid visualization of the injection process. For quantitative experiments, the number of viable bacteria injected into each embryo was estimated by dispensing the same injection volume onto solid bacteriological plates to assess bacterial counts. Injection of the bacteria onto plates was done either immediately after injecting each embryo or before and after injecting each set of 10 to 15 embryos. In the latter case, the average number of bacteria obtained for each of three plates and their standard errors of the means are presented. *M. marinum* was killed by heating an aliquot prepared as for live bacterial injections to 80°C for 15 min. Complete killing was confirmed retrospectively by plating 100 μl of

the preparation on bacteriological plates and confirming lack of growth after 7 days.

Microscopy

DIC microscopy was performed using a Nikon E600 equipped with DIC optics, 10×, 20×, and 40× magnifications, or Nikon DIC 60× Oil "plan apo" or 60× Water "fluor" objectives. Fluorescent and black and white images, including time-lapse, were collected using a Photometrics CoolSnap cf camera and processed using Universal Imaging Corp.'s Metamorph software. Color images were collected as described (Herbomel et al., 1999). Overlays of fluorescent and DIC images were produced using the Metamorph software overlay functions, with out-of-focus background fluorescence removed in some instances using Adobe PhotoShop 5.0. Composite images of several fields were assembled using Adobe PhotoShop 5.0, and time-lapse video clips were acquired as series of still images, then converted to video using Adobe Premiere 6.0. 2D reconstructions of color Z-series images (used in Figures 7C and 7D) were collected using a Sony DKC-5000 digital photo camera and assembled using Metamorph software.

Transmission Electron Microscopy

Embryos injected in the caudal vein with ~500 bacteria at 32 hr pf were processed at 6 days pi as described (Bouley et al., 2001). Ultrathin sections were cut in areas where bacteria were identified in thick sections (Bouley et al., 2001).

Expression of *M. marinum mag*s and *gag*s in Embryos

32 hr pf embryos were injected in the caudal vein with *M. marinum* bearing *mag* and *gag gfp* fusions (Chan et al., 2002). Gene fusions used were *gfp* fused to: *msp* 12 (*M. tuberculosis* Rv 3583c), *mag* 24 (*M. tuberculosis* PE-PGRS), *mag* 25 (*M. tuberculosis whiB3*), *mag 49* (*M. tuberculosis* metabolite transporter gene), *mag* 85 (*M. tuberculosis* PE gene), *gag* 7 (*M. tuberculosis recC*), *gag* 7.33 (*M. tuberculosis ald*), and *gag* 3.13 (*M. tuberculosis* Rv0133). Fluorescence of the bacteria was monitored 30 min and 2 hr pi on the first day and daily thereafter for up to 5 days pi. Each *mag* and *gag* was tested in two or three separate experiments. Fluorescence activation of individual bacteria in the aggregates was confirmed as follows: *M. marinum* expressing various *gfp* promoter fusions was used to infect J774 cells or grown in DMEM for 5 days (Ramakrishnan et al., 2000). Simultaneously, the cultures were injected into embryos via caudal vein. At day 5, after confirming that aggregates had formed in the infected embryos, individual bacteria were released by first dissociating the embryo cells using the protease treatment method (Westerfield, 2000). Bacteria were released from the dissociated cells using Triton X-100 as described for cultured cells (Ramakrishnan et al., 2000). Individual bacteria from all three conditions were examined by DIC and fluorescence microscopy. All fluorescence images were obtained with the NIKON E-600's ND4 filter and 4 s exposure time, a condition that was nonsaturating for the most fluorescent bacteria examined.

Survival in Long-Term Infections

Fifty 32 hr pf embryos were injected in the caudal vein with either wild-type or L1D *M. marinum*. The embryos were maintained in separate containers under the same conditions and monitored daily for survival along with 50 uninfected embryos. Deaths in the wild-type *M. marinum*-infected embryos were confirmed by microscopy to be due to infection. The experiment was done twice with similar results.

Microglial Cell Counts in Optic Tectum

Neutral red staining was performed as described (Herbomel et al., 2001). Macrophage accumulation in the optic tectum was examined in six uninfected embryos and six embryos injected into the caudal vein with ~500 bacteria at 72 hr pf. Average numbers of tectum macrophages and standard errors of the means were calculated and statistical analyses performed by Student's unpaired t test using Statview version 6.0. The experiment was done twice with similar results.

Acknowledgments

We thank D. Payan for suggesting zebrafish; W. Talbot, M. Hosobuchi, and N. Salama for advice and help in getting this research started; D. Raible, C. Moens, K. Urdahl, L. Zon, N. Trede, C. Cosma, S. Falkow, and J. Ernst for advice and discussions; D. Beery for fish husbandry and assistance with microscopy; O. Humbert for help with the cultured macrophage experiments; L. Swaim, G. Sanders, and members of the Kimelman and Raible laboratories, especially T. Linbo, S. Chen, and J. Lister for technical advice and help; G. Davis and E. LaChica for advice on microscopy and imaging; and M. Bevan, D. Kimelman, K. Urdahl, S. Miller, C. Petit, C. Lesser, C. Cosma, C. Darby, and T. Pozos for helpful comments on the manuscript. This work was supported by an Ellison Medical Foundation New Scholar in Global Infectious Diseases award, National Institutes of Health grant R01 AI 36396 (to L.R.), and an ACI BioDev grant from the Ministère de la Recherche (to P.H.).

Received: August 15, 2002
Revised: October 1, 2002

References

Adams, D.O. (1976). The granulomatous inflammatory response. A review. Am. J. Pathol. *84*, 164–191.

Alpuche-Aranda, C.M., Racoosin, E.L., Swanson, J.A., and Miller, S.I. (1994). *Salmonella* stimulate macrophage macropinocytosis and persist within spacious phagosomes. J. Exp. Med. *179*, 601–608.

Barker, L.P., George, K.M., Falkow, S., and Small, P.L. (1997). Differential trafficking of live and dead *Mycobacterium marinum* organisms in macrophages. Infect. Immun. *65*, 1497–1504.

Bartlett, K., Trust, T., and Lior, H. (1977). Small pet acquarium frogs as a source of *Salmonella*. Appl. Environ. Microbiol. *33*, 1026–1029.

Bean, A.G., Roach, D.R., Briscoe, H., France, M.P., Korner, H., Sedgwick, J.D., and Britton, W.J. (1999). Structural deficiencies in granuloma formation in TNF gene-targeted mice underlie the heightened susceptibility to aerosol *Mycobacterium tuberculosis* infection, which is not compensated for by lymphotoxin. J. Immunol. *162*, 3504–3511.

Bouley, D.M., Ghori, N., Mercer, K.L., Falkow, S., and Ramakrishnan, L. (2001). Dynamic nature of host-pathogen interactions in *Mycobacterium marinum* granulomas. Infect. Immun. *69*, 7820–7831.

Brennan, M.A., and Cookson, B.T. (2000). *Salmonella* induces macrophage death by caspase-1-dependent necrosis. Mol. Microbiol. *38*, 31–40.

Chan, K., Knaak, T., Satkamp, L., Humbert, O., Falkow, S., and Ramakrishnan, L. (2002). Complex pattern of *Mycobacterium marinum* gene expression during long-term granulomatous infection. Proc. Natl. Acad. Sci. USA *99*, 3920–3925.

Clark, H.F., and Shepard, C.C. (1963). Effect of environmental temperatures on infection with *Mycobacterium marinum (balnei)* of mice and a number of poikilothermic species. J. Bacteriol. *86*, 1057–1069.

Cooper, A.M., Dalton, D.K., Stewart, T.A., Griffin, J.P., Russell, D.G., and Orme, I.M. (1993). Disseminated tuberculosis in interferon gamma gene-disrupted mice. J. Exp. Med. *178*, 2243–2247.

Dannenberg, A.M., Jr. (1993). Immunopathogenesis of pulmonary tuberculosis. Hosp. Pract. *28*, 51–58.

Dooley, K., and Zon, L.I. (2000). Zebrafish: a model system for the study of human disease. Curr. Opin. Genet. Dev. *10*, 252–256.

Fenton, M.J., Vermeulen, M.W., Kim, S., Burdick, M., Strieter, R.M., and Kornfeld, H. (1997). Induction of gamma interferon production in human alveolar macrophages by *Mycobacterium tuberculosis*. Infect. Immun. *65*, 5149–5156.

Fishman, M.C. (2001). Genomics. Zebrafish–the canonical vertebrate. Science *294*, 1290–1291.

Flynn, J.L., and Chan, J. (2001). Immunology of tuberculosis. Annu. Rev. Immunol. *19*, 93–129.

Flynn, J.L., Goldstein, M.M., Chan, J., Triebold, K.J., Pfeffer, K., Lowenstein, C.J., Schreiber, R., Mak, T.W., and Bloom, B.R. (1995). Tumor necrosis factor-α is required in the protective immune re-

sponse against *Mycobacterium tuberculosis* in mice. Immunity *2*, 561–572.

Flynn, J.L., Chan, J., Triebold, K.J., Dalton, D.K., Stewart, T.A., and Bloom, B.R. (1993). An essential role for interferon gamma in resistance to *Mycobacterium tuberculosis* infection. J. Exp. Med. *178*, 2249–2254.

Golling, G., Amsterdam, A., Sun, Z., Antonelli, M., Maldonado, E., Chen, W., Burgess, S., Haldi, M., Artzt, K., Farrington, S., et al. (2002). Insertional mutagenesis in zebrafish rapidly identifies genes essential for early vertebrate development. Nat. Genet. *31*, 135–140.

Haffter, P., Granato, M., Brand, M., Mullins, M.C., Hammerschmidt, M., Kane, D.A., Odenthal, J., van Eeden, F.J., Jiang, Y.J., Heisenberg, C.P., et al. (1996). The identification of genes with unique and essential functions in the development of the zebrafish, *Danio rerio*. Development *123*, 1–36.

Haire, R.N., Rast, J.P., Litman, R.T., and Litman, G.W. (2000). Characterization of three isotypes of immunoglobulin light chains and T-cell antigen receptor alpha in zebrafish. Immunogenetics *51*, 915–923.

Herbomel, P., Thisse, B., and Thisse, C. (1999). Ontogeny and behaviour of early macrophages in the zebrafish embryo. Development *126*, 3735–3745.

Herbomel, P., Thisse, B., and Thisse, C. (2001). Zebrafish early macrophages colonize cephalic mesenchyme and developing brain, retina, and epidermis through a M-CSF receptor-dependent invasive process. Dev. Biol. *238*, 274–288.

Kaufmann, S.H., and Ladel, C.H. (1994). Role of T cell subsets in immunity against intracellular bacteria: experimental infections of knock-out mice with *Listeria monocytogenes* and *Mycobacterium bovis* BCG. Immunobiology *191*, 509–519.

Kim, D.H., Feinbaum, R., Alloing, G., Emerson, F.E., Garsin, D.A., Inoue, H., Tanaka-Hino, M., Hisamoto, N., Matsumoto, K., Tan, M.W., and Ausubel, F.M. (2002). A conserved p38 MAP kinase pathway in *Caenorhabditis elegans* innate immunity. Science *297*, 623–626.

Kimmel, C.B., Ballard, W.W., Kimmel, S.R., Ullmann, B., and Schilling, T.F. (1995). Stages of embryonic development of the zebrafish. Dev. Dyn. *203*, 253–310.

Michel, T., Reichhart, J.M., Hoffmann, J.A., and Royet, J. (2001). *Drosophila* Toll is activated by Gram-positive bacteria through a circulating peptidoglycan recognition protein. Nature *414*, 756–759.

Monack, D.M., Detweiler, C.S., and Falkow, S. (2001). *Salmonella* pathogenicity island 2-dependent macrophage death is mediated in part by the host cysteine protease caspase-1. Cell Microbiol. *3*, 825–837.

Nasevicius, A., and Ekker, S.C. (2000). Effective targeted gene 'knockdown' in zebrafish. Nat. Genet. *26*, 216–220.

North, R.J., and Izzo, A.A. (1993). Granuloma formation in severe combined immunodeficient (SCID) mice in response to progressive BCG infection. Tendency not to form granulomas in the lung is associated with faster bacterial growth in this organ. Am. J. Pathol. *142*, 1959–1966.

Ono, H., Klein, D., Vincek, V., Figueroa, F., O'hUigin, C., Tichy, H., and Klein, J. (1992). Major histocompatibility complex class II genes of zebrafish. Proc. Natl. Acad. Sci. USA *89*, 11886–11890.

Ono, H., Figueroa, F., O'hUigin, C., and Klein, J. (1993). Cloning of the beta 2-microglobulin gene in the zebrafish. Immunogenetics *38*, 1–10.

Parichy, D.M., Ransom, D.G., Paw, B., Zon, L.I., and Johnson, S.L. (2000). An orthologue of the *kit*-related gene *fms* is required for development of neural crest-derived xanthophores and a subpopulation of adult melanocytes in the zebrafish, *Danio rerio*. Development *127*, 3031–3044.

Patton, E.E., and Zon, L.I. (2001). The art and design of genetic screens: zebrafish. Nat. Rev. Genet. *2*, 956–966.

Ramakrishnan, L., Valdivia, R.H., McKerrow, J.H., and Falkow, S. (1997). *Mycobacterium marinum* causes both long-term subclinical infection and acute disease in the leopard frog (*Rana pipiens*). Infect. Immun. *65*, 767–773.

Ramakrishnan, L., Federspiel, N.A., and Falkow, S. (2000). Granuloma-specific expression of *Mycobacterium* virulence proteins from the glycine-rich PE-PGRS family. Science *288*, 1436–1439.

Ramet, M., Manfruelli, P., Pearson, A., Mathey-Prevot, B., and Ezekowitz, R.A. (2002). Functional genomic analysis of phagocytosis and identification of a *Drosophila* receptor for *E. coli*. Nature *416*, 644–648.

Remington, J., McLeod, R., and Desmonts, G. (1994). Toxoplasmosis. In Infectious Diseases of the Fetus and Newborn Infant, J. Remington and J. Klein, eds. (Philadelphia: WB Saunders).

Roach, D.R., Briscoe, H., Baumgart, K., Rathjen, D.A., and Britton, W.J. (1999). Tumor necrosis factor (TNF) and a TNF-mimetic peptide modulate the granulomatous response to *Mycobacterium bovis* BCG infection in vivo. Infect. Immun. *67*, 5473–5476.

Seeger, A., Mayer, W.E., and Klein, J. (1996). A complement factor B-like cDNA clone from the zebrafish (*Brachydanio rerio*). Mol. Immunol. *33*, 511–520.

Steyn, A.J., Collins, D.M., Hondalus, M.K., Jacobs, W.R., Jr., Kawakami, R.P., and Bloom, B.R. (2002). *Mycobacterium tuberculosis* WhiB3 interacts with RpoV to affect host survival but is dispensable for in vivo growth. Proc. Natl. Acad. Sci. USA *99*, 3147–3152.

Takeuchi, H., Figueroa, F., O'hUigin, C., and Klein, J. (1995). Cloning and characterization of class I Mhc genes of the zebrafish, *Brachydanio rerio*. Immunogenetics *42*, 77–84.

Talaat, A.M., Reimschuessel, R., Wasserman, S.S., and Trucksis, M. (1998). Goldfish, *Carassius auratus*, a novel animal model for the study of *Mycobacterium marinum* pathogenesis. Infect. Immun. *66*, 2938–2942.

Tan, M.W., and Ausubel, F.M. (2000). *Caenorhabditis elegans*: a model genetic host to study *Pseudomonas aeruginosa* pathogenesis. Curr. Opin. Microbiol. *3*, 29–34.

Teitelbaum, R., Schubert, W., Gunther, L., Kress, Y., Macaluso, F., Pollard, J.W., McMurray, D.N., and Bloom, B.R. (1999). The M cell as a portal of entry to the lung for the bacterial pathogen *Mycobacterium tuberculosis*. Immunity *10*, 641–650.

Tonjum, T., Welty, D.B., Jantzen, E., and Small, P.L. (1998). Differentiation of *Mycobacterium ulcerans*, *M. marinum*, and *M. haemophilum*: mapping of their relationships to *M. tuberculosis* by fatty acid profile analysis, DNA-DNA hybridization, and 16S rRNA gene sequence analysis. J. Clin. Microbiol. *36*, 918–925.

Travis, W.D., Travis, L.B., Roberts, G.D., Su, D.W., and Weiland, L.W. (1985). The histopathologic spectrum in *Mycobacterium marinum* infection. Arch. Pathol. Lab. Med. *109*, 1109–1113.

Trede, N.S., Zapata, A., and Zon, L.I. (2001). Fishing for lymphoid genes. Trends Immunol. *22*, 302–307.

van Crevel, R., Ottenhoff, T.H., and van der Meer, J.W. (2002). Innate immunity to *Mycobacterium tuberculosis*. Clin. Microbiol. Rev. *15*, 294–309.

Wang, J., Wakeham, J., Harkness, R., and Xing, Z. (1999). Macrophages are a significant source of type 1 cytokines during mycobacterial infection. J. Clin. Invest. *103*, 1023–1029.

Webb, S.E., Pollard, J.W., and Jones, G.E. (1996). Direct observation and quantification of macrophage chemoattraction to the growth factor CSF-1. J. Cell Sci. *109*, 793–803.

Westerfield, M. (2000). The Zebrafish Book. A Guide for the Laboratory Use of Zebrafish (*Danio rerio*). (Eugene: University of Oregon Press).

Wienholds, E., Schulte-Merker, S., Walderich, B., and Plasterk, R.H. (2002). Target-selected inactivation of the zebrafish *rag*1 gene. Science *297*, 99–102.

Willett, C.E., Zapata, A.G., Hopkins, N., and Steiner, L.A. (1997). Expression of zebrafish *rag* genes during early development identifies the thymus. Dev. Biol. *182*, 331–341.

Willett, C.E., Cortes, A., Zuasti, A., and Zapata, A.G. (1999). Early hematopoiesis and developing lymphoid organs in the zebrafish. Dev. Dyn. *214*, 323–336.